Journal of Statistical Physics, Vol. 72, Nos. 3/4, 1993

Critical Dynamics of Cluster Algorithms in the Dilute Ising Model

M. Hennecke[1,2] **and U. Heyken**[1]

Received December 8, 1992

Autocorrelation times for thermodynamic quantities at T_C are calculated from Monte Carlo simulations of the site-diluted simple cubic Ising model, using the Swendsen–Wang and Wolff cluster algorithms. Our results show that for these algorithms the autocorrelation times *decrease* when reducing the concentration of magnetic sites from 100% down to 40%. This is of crucial importance when estimating static properties of the model, since the variances of these estimators increase with autocorrelation time. The dynamical critical exponents are calculated for both algorithms, observing pronounced finite-size effects in the energy autocorrelation data for the algorithm of Wolff. We conclude that, when applied to the dilute Ising model, cluster algorithms become even more effective than local algorithms, for which *increasing* autocorrelation times are expected.

KEY WORDS: Critical phenomena; Swendsen–Wang algorithm; Wolff algorithm; critical slowing down; time series analysis, Monte Carlo error estimation.

1. INTRODUCTION

In recent years, further progress has been made in the field of Monte Carlo simulations of the Ising model with the invention of new and more effective algorithms, initiated by the work of Swendsen and Wang[1] in 1987. A variant of that method was introduced by Wolff[2] which has proved to be even more effective at criticality.[2,3] The main advantage of these algorithms is to reduce autocorrelations between successive measurements in the simulation process. This has the important consequence of reducing critical slowing down (CSD)[4] and so simplifying the simulation of larger

[1] Theoretische Physik III, Ruhr-Universität Bochum, D-44780 Bochum, Germany.
[2] Rechenzentrum, Universität Karlsruhe, D-76128 Karlsruhe, Germany.

0022-4715/93/0800-0829$07.00/0

lattices and smaller distances from the critical point. These aspects, caused by the nonlocal type of the Monte Carlo update scheme, were investigated by a variety of authors.[5–10] General reviews of attempts to reduce CSD are given by Wolff[11] and Sokal,[12] and cluster algorithms are discussed in the review of Wang and Swendsen[13] and references therein.

In this paper, we report the results of extensive simulations of the site-diluted simple cubic Ising model at concentrations $p = 1.0$, 0.8, 0.6, and 0.4. Lattices of linear dimension L ranging from 10 to 60 were simulated by the Swendsen–Wang algorithm, whereas system sizes up to $L = 75$ were used for the Wolff algorithm in order to investigate the strong finite-size effects observed in this case. The raw data recorded during the simulation are described in Section 2, together with some basic statistical prerequisites and the definition of autocorrelation times used here. Section 3 provides a survey of scaling theory and introduces the dynamical critical exponent z related to the system size dependence of autocorrelation times at criticality. Details of the simulations, the analyzing methods, and the final results are presented in Section 4. In Section 5, the performance of cluster algorithms is compared to local Monte Carlo algorithms. Section 6 concludes the article by summarizing the main results and outlining open problems.

2. STATISTICAL METHODS

The energy U and the absolute value of magnetization $|M|$ were measured during the simulation, recording one value for each Monte Carlo step per site (MCS) in the case of Swendsen–Wang and three to four values per MCS for Wolff dynamics, depending on the average size of the Wolff clusters. The time needed to flip these clusters is proportional to their mass, so the natural unit of time varies with the Wolff cluster size.

Both algorithms fulfill the detailed balance criterion,[1,2] so after equilibration the process $\{A_i\}$ with $A \in \{U, |M|\}$ should be stationary and simulate the canonical probability distribution. Observables distributed according to this probability are estimated from the simulated time series $A_1, \ldots, A_N$ with large but finite N: The estimator $\langle A \rangle$ of the mean value μ_A is calculated from

$$\langle A \rangle = \frac{1}{N} \sum_{i=1}^{N} A_i \tag{1}$$

This is an unbiased and consistent estimator of μ_A, in contrast to the estimator

$$\langle C_A(t) \rangle = \frac{1}{N-t} \sum_{i=1}^{N-t} (A_i - \langle A \rangle)(A_{i+t} - \langle A \rangle) \tag{2}$$

of the autocovariance function $C_A(t)$, which is only asymptotically $(N \to \infty)$ unbiased. The bias depends on the ratio of decay time t to simulation length N and leads to a slight underestimation of $\langle C_A(t) \rangle$, which may be neglected since $t/N < 0.001$ in this study: the deviations are too small to be observed within the resolution of our data. The estimator $\langle \rho_A(t) \rangle$ of the autocorrelation function $\rho_A(t)$ is defined by

$$\langle \rho_A(t) \rangle = \frac{\langle C_A(t) \rangle}{\langle C_A(0) \rangle} \tag{3}$$

There are different ways to define autocorrelation times:

1. The statistically relevant quantity is the integrated autocorrelation time:

$$\tau_{\text{int},A} = \tfrac{1}{2} \sum_{t=-\infty}^{\infty} \rho_A(t) = \tfrac{1}{2} + \sum_{t=1}^{\infty} \rho_A(t) \tag{4}$$

Under fairly general conditions, $\tau_{\text{int},A}$ may be used to define the *equivalent number of independent observations* in the time series and so to obtain valid variances and error bars for the estimator of the mean: the "number of observations" has to be divided by $2\tau_{\text{int},A}$ to compensate for the correlations.

When estimating $\tau_{\text{int},A}$ by substituting $\langle \rho_A(t) \rangle$ for $\rho_A(t)$, the above sum has to be truncated.[14,2] Otherwise the estimator would not be consistent, since the statistics are bad for large t. In the present analysis, the sums were truncated at the time $t_{\max}$ where $\langle \rho_A(t_{\max}+1) \rangle$ gets larger than $\langle \rho_A(t_{\max}) \rangle$, e.g., where the estimated autocorrelations become nonmonotonic.[3]

2. Exponential autocorrelation times can be introduced by postulating a multiexponential form for $\rho_A(t)$. Then $\tau_{\text{exp},A}$ is defined to be the largest relaxation time in the corresponding sum, e.g.,

$$\tau_{\text{exp},A} = \lim_{|t| \to \infty} \frac{-|t|}{\ln \rho_A(t)} \tag{5}$$

In this case, $\tau_{\text{exp},A}$ can be extracted from standard curve-fitting[16] of $\langle \rho_A(t) \rangle$ to exponential decay:

$$\langle \rho_A(t) \rangle \propto \exp(-t/\langle \tau_{\text{exp},A} \rangle) \qquad \text{(large } t\text{)} \tag{6}$$

If the approximation by a *single* exponential term is valid, both definitions give the same result, so $\tau_{\text{int},A} \approx \tau_{\text{exp},A}$. But normally there is more than one

[3] Other methods, such as self-consistent truncation windows[15] or exponential approximation of the remainder,[2] were also considered and gave similar results within error bars.

mechanism of decorrelation, so this simple exponential form might be modified to include a sum of exponentials. Then $\tau_{\text{exp},A}$ is defined to be the relaxation time of the slowest mechanism decorrelating A. With this definition, $\tau_{\text{exp},A}$ is normally larger than $\tau_{\text{int},A}$.

For a more detailed treatment of the estimation techniques summarized above, we refer to Priestley,[14] Madras and Sokal,[15] Sokal,[12] and Wolff.[2]

3. THE DYNAMICAL CRITICAL EXPONENTS

In this section, we do not note the explicit dependence on the observable A and on the definition of autocorrelation times and correlation lengths. However, if the correlation function is not a single exponential, these differences might lead to different results, e.g., different exponents. The index ∞ is used to indicate the thermodynamic limit $L \to \infty$, and finite systems are indicated by their linear dimension L.

The critical exponent[17] Δ for the *equilibrium* relaxation time τ_∞ of the physical observable A of interest is defined by the relation

$$\tau_\infty(T) \sim \hat{\tau}_\infty \cdot |\varepsilon|^{-\Delta} \qquad (T \to T_C) \tag{7}$$

where $\varepsilon = (T - T_C)/T_C$ is the relative distance from T_C. Replacing ε by using the corresponding relation for the correlation length,

$$\xi_\infty(T) \sim \hat{\xi}_\infty \cdot |\varepsilon|^{-\nu} \qquad (T \to T_C) \tag{8}$$

directly leads to the expression[4] defining the *dynamical critical exponent* z:

$$\tau_\infty(\xi_\infty(T)) \sim \hat{\tau}_\infty \cdot \xi_\infty^z, \qquad z \equiv \Delta/\nu \tag{9}$$

The dynamical critical exponent z therefore describes the dependence of the correlation time τ_∞ on the static correlation length ξ_∞, which implicitly depends on temperature. Note that using the same relation for $T < T_C$ and $T > T_C$ is only valid if a dynamic scaling assumption for the equilibrium correlations is made.[18] This implies the equivalence of the critical exponents above and below T_C.

In the infinite system, the correlation length ξ_∞ diverges for $T \to T_C$. For a finite system, ξ_L is bounded by the linear dimension L. This leads to the finite-size-scaling hypothesis for the correlation time,[19]

$$\tau_L(T) \sim L^{\Delta/\nu} \cdot \tilde{\tau}(\varepsilon^\nu L) \qquad (T \to T_C, L \to \infty) \tag{10}$$

[4] In Eq. (9), $\hat{\tau}_\infty$ also contains constants from (8) and therefore differs from the value defined in (7) by a constant.

At the critical point, the argument of the finite-size-scaling function $\tilde{\tau}(x)$ vanishes. Since $\tilde{\tau}(0)$ is a constant independent of L, for not too small L the above relation might be interpreted as

$$\tau_L(T_C) = \hat{\tau} \cdot L^z \tag{11}$$

From this relation, z can be determined by simulating systems with different linear dimensions L at T_C and plotting $\tau_L(T_C)$ as a function of L.

The theoretical knowledge on these dynamical processes *in equilibrium* is summarized in the remainder of this section. For conventional algorithms with local dynamics, the dynamical critical exponent for the *pure* Ising model was proven to fulfill the inequality[20-22]

$$z_{\text{local}} \geqslant \frac{\gamma}{\nu} \tag{12}$$

γ is the critical exponent of the susceptibility. In the case of cluster algorithms, Li and Sokal[23] obtained a rigorous lower bound

$$z_{\text{SW}} \geqslant \frac{\alpha}{\nu} \tag{13}$$

for the dynamical critical exponent of the Swendsen–Wang algorithm, where α is the critical exponent of the specific heat. Heermann and Burkitt[8] found a logarithmic system size dependence of τ by simulations of the pure Ising model in two dimensions. This shows that (13) is an equality for $d=2$, since $\alpha=0$ in this case. In the three-dimensional Ising model, all known results are larger than the lower bound $\alpha/\nu \approx 0.165$ given by Li and Sokal. Klein *et al.*[6] argue that the mechanism of domain wall diffusion which characterizes the time evolution of local algorithms is maintained in the Swendsen–Wang dynamics. Replacing the lattice spacing a giving the "size" of elementary spin flips for local algorithms by the average cluster size, they obtain the expression

$$z_{\text{SW}} = 2 - \frac{2\gamma}{d_m \nu} \tag{14}$$

with d_m being the dimension of these average (finite) clusters. This dimension is not known, but inserting as limiting values the spatial dimension $d=3$ and the fractal dimension $d_f = d - \beta/\nu \approx 2.484$ of the incipient (infinite) cluster, we obtain the bounds

$$0.41 \leqslant z_{\text{SW}} \leqslant 0.69 \tag{15}$$

which are consistent with the above rigorous lower bound and almost all numerical results. The differences between the cluster algorithms of Swendsen–Wang and Wolff are not fully understood, although it seems clear[2,3] that the proportionality of the average size of clusters flipped in the algorithm of Wolff and the susceptibility is the key to explaining the faster decorrelation in this algorithm. However, there exists no theoretical argument explaining the influence of *dilution* on the dynamics of cluster algorithms.

4. NUMERICAL RESULTS

For each set of parameters, some separate runs were performed, using different random number sequences of a shift-register random number generator[24] in the pure case and different impurity configurations in the diluted cases to obtain independent configurations for each system size: For the Swendsen–Wang algorithm, 25,000 MCS were done in five and ten runs, respectively, runs for pure and diluted systems. Autocorrelation times for the Wolff algorithm are smaller, so the length of each run was reduced to about 10,000 updates and the number of runs was extended to 10 ($p = 100\%$), 30 ($p = 80\%$ and $p = 60\%$), and 20 ($p = 40\%$) instead.[5] A total amount of 44,700 hr of processor time on a network of T800 transputers was required to perform these studies.

From Section 3 it is clear that deviations from the exact transition point lead to smaller values of z. Therefore, very good estimates for T_C are needed. For the present study, the value $T_C(100\%) = 4.51154$ for the pure Ising model[25] and the critical temperatures $T_C(80\%) = 3.496$, $T_C(60\%) = 2.418$, and $T_C(40\%) = 1.207$ given by Wang and Chowdhury[26] were used (all temperatures in units of J/k_B).

Autocorrelation function estimates $\langle \rho_A(t) \rangle$ and autocorrelation time estimates $\langle \tau_{\text{int},A} \rangle$ and $\langle \tau_{\text{exp},A} \rangle$ were calculated separately for each configuration.[6] Figure 1 shows typical autocorrelation function estimates for a dilute configuration. Averaging $\langle \tau_{\text{int},A} \rangle$ over all configurations leads to the

[5] Simulations for $p = 40\%$ were stopped after 20 configurations because of the very large fluctuations in the data, which are probably due to deviations of the estimate for $T_C(40\%)$ used from the true value.

[6] The two definitions of autocorrelation times yield different results, as should be expected if more than one exponential mode exists. It is obvious from Fig. 1 that more than one exponential mode cannot be extracted reliably. However, both integrated autocorrelation times (taking into account all exponential modes) and exponential autocorrelation times lead to comparable dynamical exponents within error bars. In the following discussion, only integrated autocorrelation times are used, since they have smaller errors and are easier to analyze.

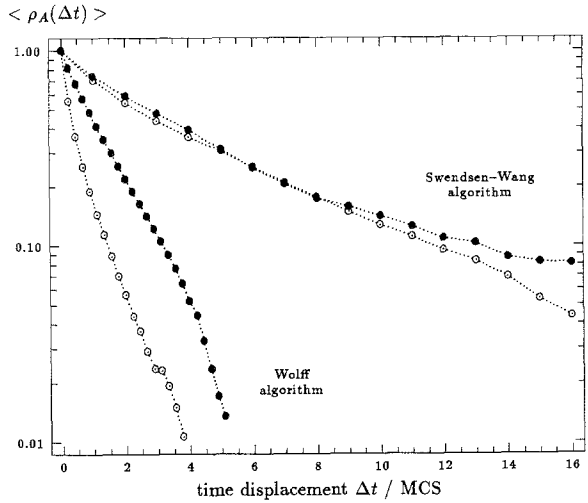

Fig. 1. Exponential decay of energy (●) and magnetization (○) equilibrium correlations for a single configuration at $p = 0.6$, $T = 2.418$, and $L = 60$.

final estimates $[\tau_{\text{int},A}]$ and $[\tau_{\text{exp},A}]$. The error bars shown in Fig. 2 and 4 are standard errors from configuration averaging, denoted by $[\cdot]$. The errors from the time-estimation procedure described in Section 2 are neglected, both because they involve four-point correlations, which are even harder to estimate by Monte Carlo simulation, and because representative investigations of simulations of various lengths showed that the influence of configurational fluctuations is much larger than the statistical errors of the time-estimation procedure.

The resulting values for $[\tau_{\text{int},A}]$ are used as a starting point to estimate the dynamical critical exponents z_A defined in Section 3. Assuming the validity of the underlying scaling assumptions, z_A is estimated by fitting $\log[\tau_{\text{int},A}]$ to $\log L$. Figure 2 shows the final results for the Swendsen–Wang algorithm; numerical values of the estimates for $\hat{\tau}_A$ and z_A are summarized in Table I. Both $\hat{\tau}_A$ and z_A decrease with dilution; corrections to finite-size scaling were only visible for $p = 1.0$ and $L \leqslant 10$. In analyzing the results for the algorithm of Wolff, we found that fits to the energy autocorrelation data are strongly influenced by the interval $[L_{\min} - L_{\max}]$ of system sizes used, whereas the results for magnetization data are independent of the system sizes within error bars. Figure 3 shows this behavior in the case $p = 1.0$ when varying the smallest system size used. Similar results were found for $p < 1.0$.

[7] For this comparison, additional data from systems of linear dimensions 6 and 8 were included.

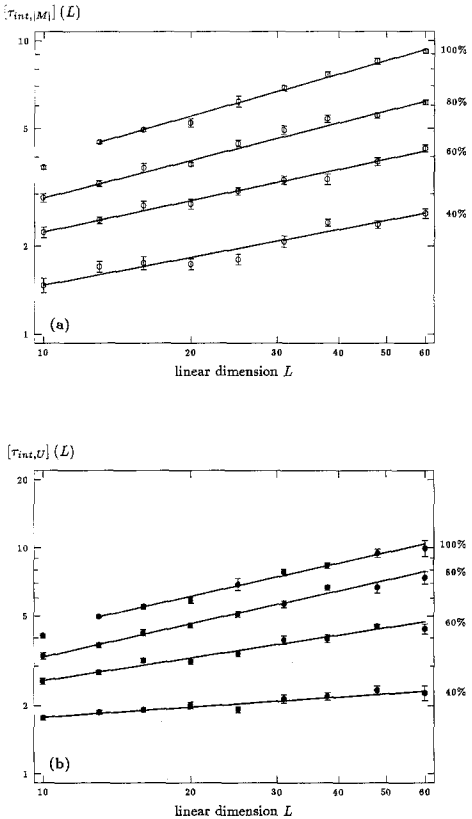

Fig. 2. Finite size scaling plots of configuration-averaged autocorrelation times for the Swendsen–Wang algorithm: (a) magnetization, (b) energy. The best fits according to Table I are indicated by solid lines. Error bars are from configuration averaging only; see text.

These findings explain the different values of the dynamical critical exponents for $p = 1.0$ given in the literature: Fitting the data for $[L = 16; L = 67]$, we obtain $z_{|M|} = 0.14 \pm 0.01$ and $z_U = 0.28 \pm 0.01$. These values are *exactly* the results obtained by Wolff[2] using system sizes from $L = 16$ to $L = 64$. Tamayo *et al.*[3] used system sizes from $L = 4$ to $L = 40$ and obtained $z = 0.44 \pm 0.1$, which is consistent with our result[7] $z_U = 0.34 \pm 0.01$ for $[L = 6; L = 38]$. We therefore conclude that the large variations of the values cited above are caused by these finite-size effects in the energy autocorrelation data. Compensating for these effects by including corrections to finite-size scaling,[19]

$$\tau_L(T_C) = \hat{\tau} \cdot L^z \{1 + \hat{C} \cdot L^{\omega}\} \tag{16}$$

Table I. Dynamical Critical Exponents z_A and Constant Factors $\hat{\tau}_A$ for the Cluster Algorithm of Swendsen and Wang[a]

p	$\hat{\tau}_{\lvert M\rvert}$	$z_{\lvert M\rvert}$	$\chi^2_{\lvert M\rvert}$	$Q_{\lvert M\rvert}$	$\hat{\tau}_U$	z_U	χ^2_U	Q_U
100%	1.32 ± 0.02	0.48 ± 0.01	5.0	0.54	1.42 ± 0.03	0.49 ± 0.02	3.1	0.79
80%	1.10 ± 0.02	0.42 ± 0.01	14.1	0.05	1.06 ± 0.03	0.49 ± 0.02	7.9	0.34
60%	0.99 ± 0.03	0.35 ± 0.02	4.4	0.73	1.19 ± 0.03	0.34 ± 0.02	13.3	0.07
40%	0.72 ± 0.03	0.31 ± 0.03	14.3	0.05	1.26 ± 0.03	0.15 ± 0.02	6.4	0.49

[a] All results are obtained by fitting the configuration averages of integrated autocorrelation time estimates to Eq. (11). The number of system sizes is 8 ($L = 13$ to $L = 60$) for $p = 1.0$ and 9 ($L = 10$ to $L = 60$) for $p < 1.0$, respectively. Errors are from weighted least-square fits; Q_A is the goodness-of-fit probability.[15]

was impossible due to the insufficient accuracy of our data. The dotted curves in Fig. 4b resulting from these attempts are only intended as guides to the eye and should not be taken seriously. In Table II, the results from fitting magnetization autocorrelations to (11) are summarized.

The values obtained for $\hat{\tau}_{|M|}(p)$ are decreasing with p, as in the case of the Swendsen–Wang algorithm. The dynamical critical exponents $z_{|M|}(p)$ for $p \neq 0.4$ do not depend systematically on p within error bars. The unreasonable small value $z_{|M|}(40\%) \approx 0.04$ is possibly caused by a too big

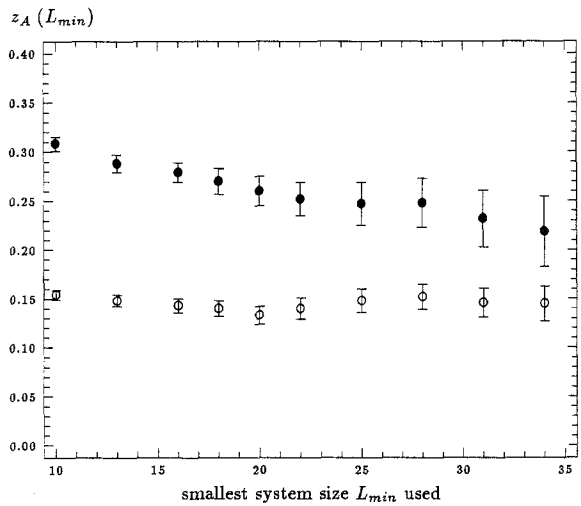

Fig. 3. Corrections to finite-size scaling for the algorithm of Wolff: Shown are estimates of $z_U(100\%)$ (●) and $z_{|M|}(100\%)$ (○) from least square fits to Eq. (11). The smallest system size $L_{\min}$ is varied as indicated; $L_{\max}$ is fixed to the largest system size simulated.

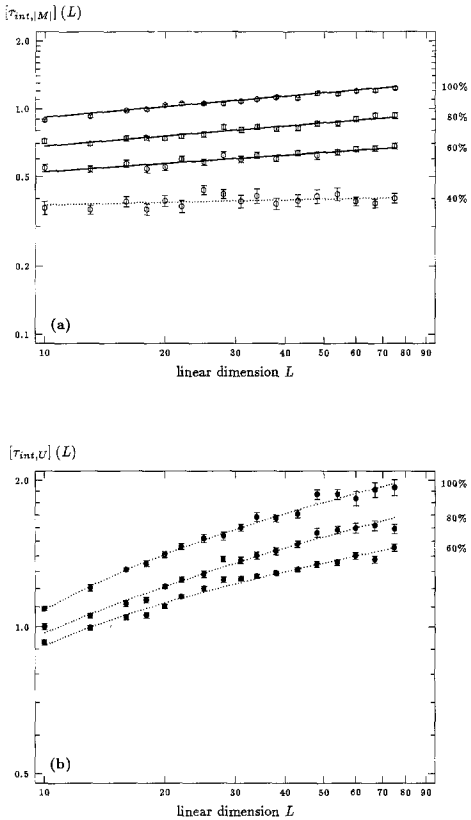

Fig. 4. Same as Fig. 2 in the case of the single cluster algorithm of Wolff. Solid curves in (a) indicate the best fits as defined by (11) and Table II. Energy autocorrelations for $p = 40\,\%$ show strong fluctuations and are therefore not shown. Dotted curves in (b) are only guides to the eye.

Table II. Dynamical Critical Exponents $z_{|M|}$ and Constant Factors $\hat{\tau}_{|M|}$ for the Single Cluster Algorithm of Wolff[a]

p	$\hat{\tau}_{\|M\|}$	$z_{\|M\|}$	$\chi^2_{\|M\|}$	$Q_{\|M\|}$
100 %	0.64 ± 0.01	0.15 ± 0.01	18.4	0.24
80 %	0.49 ± 0.01	0.15 ± 0.01	16.6	0.34
60 %	0.40 ± 0.01	0.12 ± 0.01	9.0	0.88
40 %	0.34 ± 0.01	0.04 ± 0.02	16.0	0.38

[a] All 17 system sizes from $L = 10$ to $L = 75$ were used for the fit to Eq. (11).

deviation of the value of $T_C(40\%)$ used from the real critical temperature for this concentration and should not be trusted. Consequently, the average

$$z_{1C} = 0.15 \pm 0.02 \tag{17}$$

characterizes the dynamical critical behavior of the algorithm of Wolff in the concentration range from $p = 100\%$ down to 60%.

5. COMPARISON OF ALGORITHMS

The present study was mainly motivated by the "technical" problem of checking whether or not the very fast decorrelation for cluster algorithms carries over to the dilute Ising model. Our results show that the efficiency of cluster algorithms is even improved with increasing dilution. In this section, we give some arguments which might explain the different influence of dilution on local and cluster algorithms. To show up the implications of our findings for practical Monte Carlo work, we also present a comparison of timings of a typical implementation of a vectorized local algorithm and our implementation of cluster algorithms on a parallel computer.

5.1. Theoretical Considerations

In interpreting the results of Section 4, it should be kept in mind that the dynamics of Monte Carlo simulations of the Ising model is not defined by some intrinsic *physical* time evolution, but rather by the transition matrix of the underlying Markov chain. This implies that details of the algorithm have to be considered.

The following argument might explain the influence of dilution on the value of $\tau_L(T_C(p))$: In the domain wall diffusion picture mentioned in Section 3, there are two major sources for a change of autocorrelation times with p: the correlation length (giving the typical distance a domain wall diffuses for decorrelation) and the diffusion constant (in which "speeds" of the elementary steps of the simulation algorithm enter).

The p dependence of the correlation length and the accompanying finite-size effects at $T_C(p)$ are among the unsettled problems in understanding the *static* behavior of the dilute Ising model.[8] We clearly cannot con-

[8] In the limit of weak dilution, new exponents for the dilute Ising model have been calculated: $\nu = 0.68$, $\gamma = 1.34$, and $\beta = 0.35$ in ref. 27 and $\nu = 0.671$, $\gamma = 1.321$, and $\beta = 0.348$ in ref. 28. The second case which has been analytically treated is the percolation point[29,30] $p_C \approx 0.31$; ref. 30 gives the exponents $\nu = 0.872$, $\gamma = 1.805$, and $\beta = 0.405$. All these exponents are larger than the corresponding values for the pure model[25]: $\nu = 0.630$, $\gamma = 1.241$, and $\beta = 0.325$. For intermediate values of p, no analytic theory is known. Monte Carlo simulations up to now have not reached the above limiting cases and consequently record a complex mixture from influences of probably all three sources (pure Ising, random Ising, and percolation).

tribute to these questions on the basis of our results, but we point out that changes in the correlation length are uniquely defined by the Ising model and so are *identical* for local and for cluster algorithms. Additionally, the correlation length at criticality is bounded by the linear dimension L of the system for all concentrations.[9]

The "speed" of different algorithms can be compared as follows: In local simulation algorithms, the probability to flip a single spin typically depends exponentially on the ratio of the energy difference produced by the spin flip and the temperature, so a smaller critical temperature in the dilute systems leads to exponentially smaller acceptance rates for energetically unfavorable spin flips. The consequences in reducing the temperature are opposite for cluster algorithms. The *probability* to flip a cluster in the algorithms of Swendsen–Wang and Wolff is 50% and 100%, respectively, independent of temperature. The *size* of clusters is determined by the probability of activating bonds which constitute these clusters.[2,3] This bond probability is greater than zero only for bonds between parallel spins, in which case it is given by

$$p_{\text{act}} = 1 - \exp\left\{-\frac{2J}{k_B T}\right\} \tag{18}$$

with ferromagnetic exchange coupling $J > 0$ and Boltzmann's constant k_B. This expression leads to *increasing* cluster sizes when reducing temperature.[10]

This argument might explain the autocorrelation time results for fixed L presented in Section 4. Our hypothesis of increasing autocorrelation times at $T_C(p)$ for *local* dynamics was supported recently by local Monte Carlo simulations.[32] The system size dependence of autocorrelation times (and the corresponding exponent z) is *not* explained by this reasoning. The above argument only applies to the magnitudes of autocorrelations *at fixed* L, and without precise knowledge of the changes in the static behavior, any explanation of the values of z observed could hardly be justified.

[9] However, these bounds might differ by p-dependent factors which are irrelevant for the finite-size analysis, but may be important for comparing the amplitudes $\tau_L(T_C(p))$ for fixed L and varying p.

[10] The "thinning" of the lattice is only linear $[(1/T_C)\, dT_C(p)/dp \approx 1$ in the range of concentrations used[31]], whereas the activation probability increases exponentially. The net effect should therefore be a larger cluster size.

5.2. Comparison of Implementations

We present a comparison of typical implementations of the algorithms considered above in this subsection.[11] The "physical" parameters for the comparison are our results for cluster algorithms summarized in Tables I and II, and the results of Heuer[32] for local methods. The data in ref. 32 show that for local algorithms, autocorrelation times *and* the dynamical critical exponent z increase, from $\tau_L(T_C(100\%)) \approx 0.051 L^{2.10}$ in the pure system to $\tau_L(T_C(60\%)) \approx 0.017 L^{2.93}$ for the dilution $p = 0.6$.

The "technical" and strongly implementation-dependent parameter is the speed of the programs in MCS per second. Ref. 32 is based on a vectorized program on Cray Y-MP with 335×10^6 MCS per second for $p = 1.0$ and 215×10^6 MCS per second for $p < 1.0$, which is one of the fastest programs on vector computers. The present study was done on a transputer array with T800 processors (25 MHz), with update speeds of roughly $13.8 \times 10^3 * p$ MSC per second and processor for the Swendsen–Wang algorithm and $12.5 \times 10^3 / p$ MSC per second and processor for the algorithm of Wolff.[12]

The number of effectively uncorrelated measurements per second can be calculated with the data mentioned above by the following expression:

$$N_{\text{eff}} = \frac{MCS(p, \text{program})}{2\hat{\tau}(p)} \cdot L^{-[3+z(p)]} \tag{19}$$

Figure 5 shows the results for $p = 1.0$ and $p = 0.6$. To demonstrate the possibility to increase the performance of parallel computers by adding more processors, the results for cluster algorithms are shown as a whole region of speeds corresponding to 8 up to 64 transputers.

Obviously, the simulation speeds for the pure Ising model show that fast vectorized local methods have the best performance for linear dimensions up to $L = 60$ for $p = 1.0$. Above $L = 60$, the algorithm of Wolff performs better when run on a sufficiently large transputer network, e.g., a 64-processor SuperCluster. It is also clear from Fig. 5 that the algorithm of Wolff is to be preferred to the Swendsen–Wang algorithm, which is faster than local methods only for some $L > 200$. This is caused by the different

[11] Because of the following difficulties, only *magnetization* data are used: Two recent studies using local methods[21,33] both lead to $z \approx 2$ for the pure Ising model, but energy autocorrelation times differ by a factor of three, which is not understood yet. Additionally, the energy autocorrelations for the algorithm of Wolff found in the present paper are strongly influenced by finite-size effects, as discussed in Section 4.

[12] The *increase* of performance with dilution is caused by the fact that the single cluster construction algorithm mainly operates on occupied sites.

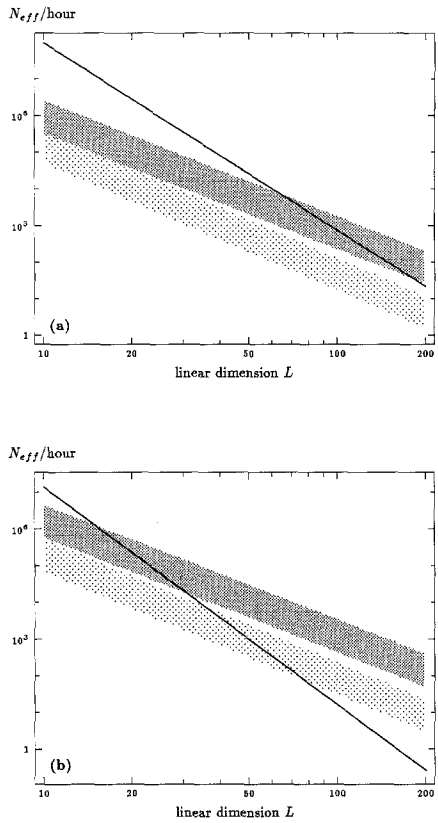

Fig. 5. Number of effectively uncorrelated measurements N_{eff} per hour CPU time for different simulation algorithms: (a) pure system, (b) dilute system, $p = 60\%$. Solid lines: local algorithm on Cray Y-MP 832, from ref. 32. Dark shaded: Wolff's algorithm. Light shaded: Swendsen–Wang algorithm. Both cluster algorithms are shown from 8 (bottom) to 64 (top) T800 transputers.

values of z, program speeds for cluster algorithms being of the same order. For the simulations at $p = 60\%$, cluster algorithms are definitely faster than local methods, even for the (small) system sizes typically studied in the past.

6. CONCLUSIONS

The main result of this study clearly is the fact that for fixed system size L, autocorrelation times at $T_C(p)$ are *decreasing* with dilution. At least for the Swendsen–Wang algorithm, the dynamical critical exponent also

decreases with increasing dilution. This behavior is contrary to the results for local algorithms, as revealed in ref. 32. The practical consequence of this phenomenon is that for Monte Carlo simulations of the dilute Ising model (or of large pure systems), cluster algorithms are to be preferred to vectorized local algorithms, at least if they can be run on scalable parallel machines.

The arguments presented in Section 5 reveal some differences of the two types of algorithms and explain the p dependence of autocorrelation times at fixed L. To obtain a deeper insight into the underlying mechanisms, it is a necessary prerequisite that the static properties of the dilute Ising model be much better understood. To answer the open questions concerning the dynamical critical exponents, the algorithm of Wolff should be run on much larger systems and the dynamic correlation function itself requires further investigation. Finally, the fact that z_{local} increases and z_{SW} decreases with dilution indicates that dynamic universality is not completely determined by the static universality class.

ACKNOWLEDGMENTS

We would like to thank M. Podgórny for many useful discussions on numerical methods and W. Bathelt for his help with some Fortran programs. We also thank H. O. Heuer for discussion and comments on the final form of the manuscript, A. Sokal for correspondence, and U. Wolff for providing a copy of ref. 11.

REFERENCES

1. R. H. Swendsen and J. S. Wang, Nonuniversal critical dynamics in Monte Carlo simulations, *Phys. Rev. Lett.* **58**:86–88 (1987).
2. U. Wolff, Comparison between cluster Monte Carlo algorithms in the Ising model, *Phys. Lett. B* **228**:379–382 (1989).
3. P. Tamayo, R. C. Brower, and W. Klein, Single-cluster Monte Carlo dynamics for the Ising model, *J. Stat. Phys.* **58**:1083–1094, **60**:899 (1990).
4. P. C. Hohenberg and B. I. Halperin, Theory of dynamic critical phenomena, *Rev. Mod. Phys.* **49**:435–479 (1977).
5. M. D'Onorio De Meo, D. W. Heermann, and K. Binder, Monte Carlo studies of the Ising model phase transition in terms of the percolation transition of physical clusters, *J. Stat. Phys.* **60**:585–618 (1990).
6. W. Klein, T. Ray, and P. Tamayo, Scaling ansatz for Swendsen–Wang dynamics, *Phys. Rev. Lett.* **62**:163–165 (1989).
7. J. S. Wang, Critical dynamics of the Swendsen–Wang algorithm in the three-dimensional Ising model, *Physica A* **164**:240–244 (1990).
8. D. W. Heermann and A. N. Burkitt, System size dependence of the autocorrelation time for the Swendsen–Wang Ising model, *Physica A* **162**:210–214 (1990).

9. T. S. Ray, P. Tamayo, and W. Klein, Mean-field study of the Swendsen–Wang dynamics, *Phys. Rev. A* **39**:5949–5953 (1989).
10. P. Tamayo and W. Klein, Critical dynamics and global conservation laws, *Phys. Rev. Lett.* **63**:2757–2759 (1989).
11. U. Wolff, Critical slowing down, in LATTICE '89 Symposium on Lattice Field Theory, Capri, Italy; Bielefeld Preprint BI-TP 89/35 (November 1989).
12. A. D. Sokal, New numerical algorithms for critical phenomena, in *Computer Studies in Condensed Matter Physics* (Springer, Berlin, 1988), pp. 6–18.
13. J. S. Wang and R. H. Swendsen, Cluster Monte Carlo algorithms, *Physica A* **167**:565–579 (1990).
14. M. B. Priestley, *Spectral Analysis and Time Series* (Academic Press, London, 1981).
15. N. Madras and A. D. Sokal, The Pivot algorithm: A highly efficient Monte Carlo method for the self-avoiding walk, *J. Stat. Phys.* **50**:109–186 (1988).
16. W. H. Press, B. P. Flannery, S. A. Teukolsky, and W. T. Vetterling, *Numerical Recipes in C: The Art of Scientific Computing* (Cambridge University Press, Cambridge, 1988).
17. E. Stanley, *Introduction to Phase Transitions and Critical Phenomena* (Clarendon Press, Oxford, 1971).
18. A. Hankey and H. E. Stanley, Systematic application of generalized homogeneous functions to static scaling, dynamic scaling and universality, *Phys. Rev. B* **6**:3515–3542 (1972).
19. M. N. Barber, Finite-size scaling, in *Phase Transitions and Critical Phenomena*, Vol. 8 (Academic Press, London, 1983).
20. S. Wansleben and D. P. Landau, Dynamical critical exponent of the 3D Ising model, *J. Appl. Phys.* **61**:3968–3970 (1987).
21. S. Wansleben and D. P. Landau, Monte Carlo investigation of critical dynamics in the 3D Ising model, *Phys. Rev. B* **43**:6006–6014 (1991).
22. B. I. Halperin, Rigorous inequalities for the spin-relaxation function in the kinetic Ising model, *Phys. Rev. B* **8**:4437–4440 (1973).
23. X. J. Li and A. D. Sokal, Rigorous lower bound on the dynamic critical exponents of the Swendsen–Wang algorithm, *Phys. Rev. Lett.* **63**:827–830 (1989).
24. S. Kirkpatrick and E. Stoll, A very fast shift-register sequence random number generator, *J. Computational Phys.* **40**:517–526 (1981).
25. J. C. Le Guillou and J. Zinn-Justin, Critical exponents from field theory, *Phys. Rev. B* **21**:3976–3998 (1980).
26. J. S. Wang and D. Chowdhury, The critical behaviour of the three-dimensional dilute Ising model: Universality and the Harris criterion, *J. Phys.* (Paris) **50**:2905 (1989).
27. G. Jug, Critical behaviour of disordered spin systems in two and three dimensions, *Phys. Rev. B* **27**:609–612 (1983).
28. I. O. Mayer, Critical exponents of the dilute Ising model from four-loop expansions, *J. Phys. A* **22**:2815–2823 (1989).
29. A. Coniglio, Thermal phase transition of the dilute s-state Potts and n-vector models at the percolation threshold, *Phys. Rev. Lett.* **46**:250–253 (1981).
30. J. Adler, Y. Meir, A. Aharony, and A. B. Harris, Series study of percolation moments in general dimension, *Phys. Rev. Lett.* **46**:250–253 (1981).
31. R. B. Stinchcombe, Dilute magnetism, in *Phase Transitions and Critical Phenomena*, Vol. 7 (Academic Press, London, 1983).
32. H. O. Heuer, Dynamic scaling of disordered Ising systems, Preprint, 25.09.1992.
33. H. O. Heuer, Critical slowing down in local dynamics simulation, *J. Phys. A* **25**:L567–L573 (1992).